10286 *Biochemistry* **2009,** *48,* 10286–10297
DOI: 10.1021/bi9013775

BIOCHEMISTRY
including biophysical chemistry & molecular biology
Article

GPR37 Surface Expression Enhancement via N-Terminal Truncation or Protein−Protein Interactions[†]

Jill H. Dunham, Rebecca C. Meyer, Erin L. Garcia, and Randy A. Hall*

Department of Pharmacology, Emory University School of Medicine, Atlanta, Georgia 30322

Received August 7, 2009; Revised Manuscript Received September 30, 2009

ABSTRACT: GPR37, also known as the parkin-associated endothelin-like receptor (Pael-R), is an orphan G-protein-coupled receptor (GPCR) that exhibits poor plasma membrane expression when expressed in most cell types. We sought to find ways to enhance GPR37 trafficking to the cell surface to facilitate studies of GPR37 functional activity in heterologous cells. In truncation studies, we found that removing the GPR37 N-terminus (NT) dramatically enhanced the receptor's plasma membrane insertion. Further studies on sequential NT truncations revealed that removal of the first 210 amino acids increased the level of surface expression nearly as much as removal of the entire NT. In studies examining the effects of coexpression of GPR37 with a variety of other GPCRs, we observed significant increases in the level of GPR37 surface expression when the receptor was coexpressed with adenosine receptor $A_{2A}R$ or dopamine receptor D_2R. Co-immunoprecipitation experiments revealed that full-length GPR37 and, to a greater extent, the truncated GPR37 were capable of robustly associating with D_2R, resulting in modestly altered D_2R affinity for both agonists and antagonists. In studies examining potential interactions of GPR37 with PDZ scaffolds, we observed a specific interaction between GPR37 and syntenin-1, which resulted in a dramatic increase in the level of GPR37 surface expression in HEK-293 cells. These findings reveal three independent approaches (N-terminal truncation, coexpression with other receptors, and coexpression with syntenin-1) by which GPR37 surface trafficking in heterologous cells can be greatly enhanced to facilitate functional studies with this orphan receptor.

The orphan G-protein-coupled receptor (GPCR)[1] GPR37, also known as the parkin-associated endothelin-like receptor (Pael-R), is strongly expressed in the mammalian central nervous system, but its function still remains largely unknown. GPR37 is most closely related to another CNS-enriched orphan receptor known as GPR37-like 1 (GPR37L1), and both orphans share significant sequence homology with the endothelin B receptor and other related peptide-activated GPCRs (*1*−*5*). However, none of the mammalian peptides tested so far, including endothelins, bombesin, and others, have produced activation of any signaling pathways in heterologous cells or *Xenopus* oocytes expressing either GPR37 or GPR37L1 (*2*−*5*). A peptide called "head activator" (HA), which is derived from the freshwater coelenterate *Hydra*, has been reported to be capable of activating GPR37 (*6*), but no peptide equivalent to HA has been definitively identified in vertebrates. Thus, GPR37 and GPR37L1 must still be considered orphan GPCRs at present.

A major stumbling block impeding progress in understanding the ligand binding and signaling of GPR37 is the receptor's poor trafficking to the plasma membrane in most heterologous cell lines. GPR37 is commonly misfolded and therefore aggregated in the endoplasmic reticulum (ER) (*1*, *7*−*9*). The E3 ubiquitin ligase parkin ubiquitinates misfolded GPR37 in the ER, targeting it for degradation and thus preventing detrimental aggregation. Mutations to parkin, observed in postmortem brain tissue of patients with autosomal recessive juvenile Parkinson's disease (AR-JP), inhibit proper functioning of parkin (*1*). It is believed that these mutations allow for aggregation of GPR37 along with other parkin substrates, leading to significant ER stress and eventually neuronal cell death (*1*, *7*−*9*). Additionally, GPR37 knockout (KO) mice are resistant to MPTP-induced neurotoxicity, a commonly used animal model of Parkinson's disease (PD) (*10*). Moreover, autophagosome accumulations are found in brain samples of patients with PD, and recent findings suggest that overexpression of GPR37 can induce autophagy (*9*). These findings suggest that GPR37 may play a role in the pathology of PD, which enhances the importance of gaining insight into the trafficking and signaling of this orphan receptor.

Other GPCRs that exhibit trafficking defects in heterologous cells, including $GABA_BR1$ (*11*−*15*), the CB1 cannabinoid receptor (*16*), and the α_{1D}-adrenergic receptor (*17*−*20*), have been shown to be more efficiently transported following truncations of either the receptor's N-terminal (NT) or C-terminal (CT) region (*21*). Thus, in the studies reported here, we created truncated forms of GPR37 to shed light on specific regions of GPR37 that influence its plasma membrane expression. Moreover, since interactions between GPCRs have been shown in some cases to strongly influence receptor surface expression and functional activity (*21*−*25*), we examined the capacity of GPR37 to

[†]This work was supported by Pharmacological Sciences Training Grant T32 GM008602, the National Institutes of Health, and the W. M. Keck Foundation.

*To whom correspondence should be addressed: Rollins Research Center, Room 5113, 1510 Clifton Rd., Atlanta, GA 30322. Phone: (404) 727-3699. Fax: (404) 727-0365. E-mail: rhall@pharm.emory.edu.

[1]Abbreviations: Pael-R, parkin-associated endothelin-like receptor; GPCR, G-protein-coupled receptor; NT, N-terminus; HA, head activator; ER, endoplasmic reticulum; AR-JP, autosomal recessive juvenile Parkinson's disease; KO, knockout; PD, Parkinson's disease; CT, C-terminal; wt, wild-type; GST, glutathione *S*-transferase; HEK, human embryonic kidney; PFA, paraformaldehyde; BSA, bovine serum albumin; FBS, fetal bovine serum; SEM, standard error of the mean.

 Published on Web 10/02/2009

associate with other GPCRs. Finally, because PDZ scaffolds have the capacity to affect surface expression of certain receptors (*21*, *26*), we examined the capacity of the GPR37 CT to interact with PDZ scaffold proteins. Our studies have revealed that removal of a portion of the GPR37 NT results in a dramatic enhancement of receptor surface expression, that coexpression with certain other receptors enhances trafficking of GPR37 to the plasma membrane, and that interactions with the PDZ scaffold protein syntenin-1 promote GPR37 surface expression.

MATERIALS AND METHODS

Materials. Materials were obtained from the following sources: human embryonic kidney 293 (HEK-293) cells (ATCC, Manassas, VA); HA-A_{2A}R, HA-A_{2B}R, EE-$G\alpha_{i1}$, EE-$G\alpha_q$, GPR37, HA-NPY_1R, HA-NPY_2R, HA-D_2R, and HA-D_1R (Missouri S&T cDNA Resource Center, Rolla, MO); FLAG-GPR37L1 (Multispan, Hayward, CA); Dulbecco's modified Eagle's medium (DMEM), Lipofectamine 2000, precast 4 to 20% Tris-glycine gels, AlexaFluor 488 and 800 goat anti-mouse antibodies, and AlexaFluor 546 and 700 goat anti-rabbit antibodies (Invitrogen, Carlsbad, CA); anti-FLAG M2 monoclonal antibody, forskolin, isoproterenol, haloperidol, butaclamol, dopamine, (−)-quinpirole hydrochloride, cAMP, GDP, GTP, and anti-FLAG M2 agarose (Sigma, St. Louis, MO); complete protease inhibitors, anti-HA 3F10 polyclonal antibody, and anti-HA 12CA5 monoclonal antibody (Roche, Indianapolis, IN); DAPI (AppliChem, Ottoweg, Darmstadt, Germany); ECL anti-mouse IgG, horseradish peroxidase-linked whole antibody, [^{3}H]cAMP, and [^{3}H]spiperone (GE Healthcare, Buckinghamshire, U.K.); anti-Na^+/K^+ ATPase antibody (Upstate/Millipore, Billerica, MA); penicillin/streptomycin solution, bovine serum albumin (BSA), and ScintiSafe scintillation fluid (Fisher, Herndon, VA); fetal bovine serum (FBS) (Atlanta Biologicals, Atlanta, GA); QuickChange XL site-directed mutagenesis kit (Stratagene, Cedar Creek, TX); head activator neuropeptide (Phoenix Pharmaceuticals, Belmont, CA, and Bachem AG, Bubendorf, Switzerland); SuperSignal Elisa Pico ECL reagent (Pierce, Rockford, IL); nitrocellulose membranes (Bio-Rad, Hercules, CA); Brandel filters (Brandel Inc., Gaithersburg, MD); p44/42 MAPK (ERK1/2) rabbit antibody and immobilized phsopho-p44/42 MAPK (ERK1/2) mouse antibody (Cell Signaling Technology, Danvers, MA); [^{3}H]YM-019151-2 (Perkin-Elmer, Waltham, MA); [^{3}H]adenine and [^{3}H]adenosine (American Radiolabeled Chemicals, Inc., St. Louis, MO).

Cell Culture and Transfection. HEK-293 cells were maintained in DMEM supplemented with 10% FBS and a 1% penicillin/streptomycin solution at 37 °C with 5% CO_2. Cells in 10 cm tissue culture dishes at a confluency of 50−60% were transfected with 1−3 μg of cDNA mixed with 15 μL of Lipofectamine 2000 in 5 mL of serum-free medium. Following a 4−5 h incubation, complete medium was added to stop the transfection. The cDNAs used were FLAG-GPR37 in pCMV2b, FLAG-GPR37L1 in pMEX2, ΔCT, Δ^{1-35}, Δ^{1-70}, Δ^{1-105}, Δ^{1-140}, Δ^{1-175}, Δ^{1-210}, and Δ^{1-255} FLAG-GPR37 in pCMV2b, 3xHA-D_2R, 3xHA-A_{2A}, and A_{2B}R, EE-tagged $G\alpha_o$ and $G\alpha_q$ and HA-NPYR 1 and 2 in pCDNA3.1 (+), DAT in pcDNA3.1 (−)/Neo, syntenin-1 in pMT-HA vector, and empty pCMV2b vector. All cDNAs used were human.

Surface Luminometer Assay. HEK-293 cells transiently transfected with FLAG-tagged or HA-tagged constructs were split into poly-D-lysine-coated 35 mm dishes and grown overnight at 37 °C. For internalization assays, ligand was added into incomplete medium and placed on cells for 30−60 min at 37 °C. The cells were washed with phosphate-buffered saline (PBS+Ca^{2+}), fixed for 30 min with 2% paraformaldehyde (PFA), and washed with PBS+Ca^{2+} again. The cells were then incubated in blocking buffer [2% nonfat dry milk in PBS (pH 7.4)] for 30 min at room temperature (RT), followed by RT incubation with horseradish peroxidase-conjugated M2 anti-FLAG antibody (1:1000) or 12CA5-anti-HA antibody (1:1000) in blocking buffer for 1 h. For tracking HA-tagged receptors, cells were washed and incubated with anti-mouse IgG, horseradish peroxidase-linked whole antibody (1:2500) for 30 min at RT. The cells were washed twice with blocking buffer, washed once with PBS+Ca^{2+}, and incubated with SuperSignal Pico ECL reagent for 15 s. The luminescence of the entire 35 mm dish was determined using a TD20/20 luminometer (Turner Designs).

Flow Cytometry. HEK-293 cells that had been transiently transfected were split into poly-D-lysine-coated 35 mm dishes and grown overnight at 37 °C. The cells were transferred to ice, washed with PBS+Ca^{2+} once, and incubated with M2 anti-FLAG antibody (1:300) in 1% BSA for 1 h. Then, the cells were washed once and incubated in the dark with Alexa Fluor 488 antimouse antibody (1:500) in 1% BSA for 1 h. Again, the cells were washed once, incubated for 15 min with 10 mM Tris and 5 mM EDTA, shaken loose, and transferred to tubes containing an equal volume of 4% PFA. Samples were spun down, and the supernatant was aspirated and resuspended in 250 μL of 1% BSA. Flow cytometric acquisition and analysis were performed on at least 10000 acquired events on an LSR II flow cytometer driven by FACSDiva (BD Biosciences). Data analysis was performed using FlowJo (Tree Star).

Mutagenesis. Six forward primers and one reverse primer were designed to make sequential truncations of GPR37. Truncated constructs were generated via PCR using those primers and a cDNA corresponding to full-length GPR37. The PCR products were digested with *Bam*HI and *Eco*RI and inserted into previously digested pCMV-2B, containing an N-terminal FLAG epitope. All sequences of truncated receptors were confirmed by sequence analysis (Agencourt, Beverly, MA).

Western Blotting. Samples were resolved by SDS−PAGE on 4 to 20% Tris-glycine gels, followed by transfer to nitrocellulose membranes. The membranes were incubated in blocking buffer (2% nonfat dry milk, 50 mM NaCl, 20 mM HEPES, and 0.1% Tween 20) for 30 min and then incubated with primary antibody either for 1 h at RT or overnight at 4 °C. Next, the membranes were washed three times in blocking buffer and incubated with either a fluorescent or HRP-conjugated secondary antibody for 30 min, washed three times more, and finally visualized using either the Odyssey imaging system (Li-Cor) or via ECL reagent followed by exposure to film.

Confocal Microscopy. Cells transiently transfected with FLAG-tagged constructs were grown on poly-D-lysine-coated glass slides. The cells were rinsed with PBS+Ca^{2+}, fixed with 2% PFA at RT, and washed three times with PBS+Ca^{2+}. Fixed cells were permeabilized and blocked via incubation for 30 min at RT in saponin buffer (1% BSA, 0.08% saponin, and PBS+Ca^{2+}). Next, the cells were washed three times and incubated with rabbit anti-FLAG antibody (1:1000) and anti-Na^+/K^+ ATPase (1:500) in 1% BSA at 37 °C for 1 h. After being washed twice with PBS+Ca^{2+}, cells were incubated in the dark with Alexa Fluor anti-mouse 488 and anti-rabbit 546 antibodies (1:250) in 1% BSA

for 1 h at RT. Cells were washed two more times for 5 min with PBS+Ca^{2+}, stained with DAPI for 10 min, rinsed twice with water, and mounted with Vectashield mounting medium. Cells were examined using a Zeiss LSM 510 laser scanning confocal microscope. For MATLAB analysis, confocal images were saved as Photoshop files. The plasma membrane regions were then outlined, and a section of the background of each image was also outlined to be subtracted from the signal as nonspecific binding. A MATLAB (Mathworks, Natick, MA) program was then used to analyze all cells to quantify the amount of receptor (red) on the cell surface (green).

Immunoprecipitation Studies. Transiently transfected HEK-293 cells were harvested by being washed once in ice-cold PBS and scraped in harvest buffer [10 mM HEPES, 100 mM NaCl, 5 mM EDTA, 1 mM benzamidine, protease inhibitor tablet, and 1% Triton X-100 (pH 7.4)]. Cell lysates were then solubilized, immunoprecipitated with anti-FLAG M2 affinity resin or protein A/G beads with anti-HA 3F10, and washed by repeated centrifugation and homogenization. Samples were heated and then probed via Western blotting using anti-FLAG M2 or anti-HA 3F10 antibodies.

Ligand Binding Studies. For the preparation of cell lysates to be used in ligand binding assays, transfected cells grown on 100 mm dishes were rinsed with 2 mL of PBS+Ca^{2+} and then starved for 1 h in 5 mL of PBS+Ca^{2+}. The cells were scraped into 1 mL of ice-cold binding buffer [20 mM HEPES, 100 mM NaCl, 5 mM $MgCl_2$, 1.5 mM CaCl, 5 mM KCl, 0.5 mM EDTA, and protease inhibitor tablet (pH 7.4)]. Cells were frozen at −20 °C until they were used. On the day of the assay, cells were thawed and centrifuged at 13500 rpm for 15 min to separate membranes. Membranes were then resuspended in 1 mL of binding buffer, triturated, and incubated with increasing concentrations of unlabeled ligands in the presence of 0.5 nM [^{3}H]spiperone to generate competition curves. The samples were incubated for 1 h at 25 °C. Nonspecific binding was defined as [^{3}H]spiperone binding in the presence of 50 μM (+)-butaclamol and represented less than 10% of total binding in all experiments. Incubations were terminated via filtration through GF/C filter paper, previously soaked in a 0.05% polyethyleneimine solution, using a Brandel cell harvester. On the harvester, filters were rapidly washed three times with ice-cold wash buffer (10 mM HEPES and 50 mM NaCl), and radioactive ligand retained by the filters was quantified via liquid scintillation spectrometry. The fitting of curves for one site versus two sites was performed, and the goodness of fit was quantified using F tests, comparing sum-of-squares values for the one-site versus two-site fits.

Purification of Fusion Proteins. Wild-type and mutant (removal of final cysteine) GST-tagged constructs (termed GPR37-CT and GPR37-Mut-CT, respectively) were created by PCR followed by insertion into the pGEX-4T1 vector. Overnight cultures of BL-21 DE Gold cells transformed with pGEX-4T1, pGEX-4T1-CT, or pGEX-4T1-Mut were diluted 1:143 into 1 L of LB broth supplemented with appropriate antibiotics and grown to an optical density (A_{600}) of 0.6−0.7 at 37 °C. IPTG was then added to the culture and allowed to incubate for 2 h. Bacteria were pelleted by centrifugation, and the GST, GPR37-CT−GST, or GPR37-Mut−GST proteins were purified using Sigma GSH agarose. The fusion proteins remained attached to GST agarose for the syntenin-1 pull-down or were eluted for use in overlays of the PDZ array. Eluted proteins were concentrated using the Amicon Ultra protein concentration system via centrifugation at 4 °C to remove excess glutathione, and the concentrations of the purified proteins were determined by the QuickStart Bradford protein assay according to the manufacturer's protocols (Bio-Rad).

Fusion Protein Pull-Down Assays. HEK-293 cells transiently transfected with HA-syntenin-1 (kindly provided by P. Coffer, UMC Utrecht, Utrecht, The Netherlands) were harvested in a detergent-free harvest buffer (10 mM HEPES, 50 mM NaCl, 5 mM EDTA, and protease inhibitor tablet). The cells were spun down to isolate the membranes, which were then incubated in harvest buffer containing 1% Triton X-100 for 1 h at 4 °C with end-over-end agitation. The samples were spun down again to separate the soluble lysates from the insoluble material. A sample of the solubilized protein was retained to ensure syntenin-1 expression and solubilization. The remaining lysates were divided evenly and incubated with glutathione−agarose beads loaded with GST, GPR37-CT−GST, or GPR37-Mut−GST proteins end over end for 1 h at 4 °C. The beads were washed five times with harvest buffer containing 1% Triton X-100 and then heated in sample buffer to strip proteins from the beads. The samples were then analyzed via Western blot for pull-down of syntenin-1 using an anti-HA antibody.

Statistical Analysis. All statistical analyses were carried out using GraphPad Prism (GraphPad Software Inc., San Diego, CA).

RESULTS

N-Terminal Truncation of GPR37 Increases the Level of Plasma Membrane Expression. HEK-293 cells were transfected with FLAG-tagged GPR37 (Figure 1A) or GPR37L1 (Figure 1B). Plasma membrane trafficking of the receptors was assessed using three independent techniques: a quantitative luminometer-based assay, FACS analysis, and confocal microscopy. In the luminometer-based surface expression assays, very little plasma membrane expression of GPR37 was observed, consistent with previous reports (*1*, *6*, *8*, *27*). In contrast, GPR37L1 was robustly transported to the plasma membrane (Figure 1C). FACS analysis confirmed that GPR37L1 was strongly expressed on the cell surface, whereas GPR37 expression was barely detectable (Figure 1D) despite comparable levels of Western blot staining for the two receptors (data not shown). To confirm these findings via a third independent technique, confocal microscopy studies were performed using the Na^+/K^+ ATPase as a plasma membrane marker. As shown in the representative images in Figure 1, mainly punctate intracellular staining was observed for GPR37 (Figure 1E), whereas GPR37L1 was predominantly localized at the plasma membrane (Figure 1F). MATLAB analysis of the images revealed that approximately 42% of the overall transfected GPR37L1 exhibited cell surface expression, whereas the cell surface expression for wt GPR37 was undetectable by these methods (< 1%). Thus, despite the high degree of sequence similarity between the two receptors, GPR37L1 exhibited robust surface expression in our studies whereas GPR37 was weakly transported to the plasma membrane.

Given the striking difference in plasma membrane expression between GPR37 and GPR37L1, we next focused on determining which region of these related receptors might account for this difference. GPR37L1 shares 68% homology and 48% identity with GPR37, with most of the sequence identity concentrated in the receptors' transmembrane regions (*3*, *5*). Since the main differences between the two receptors are found in their

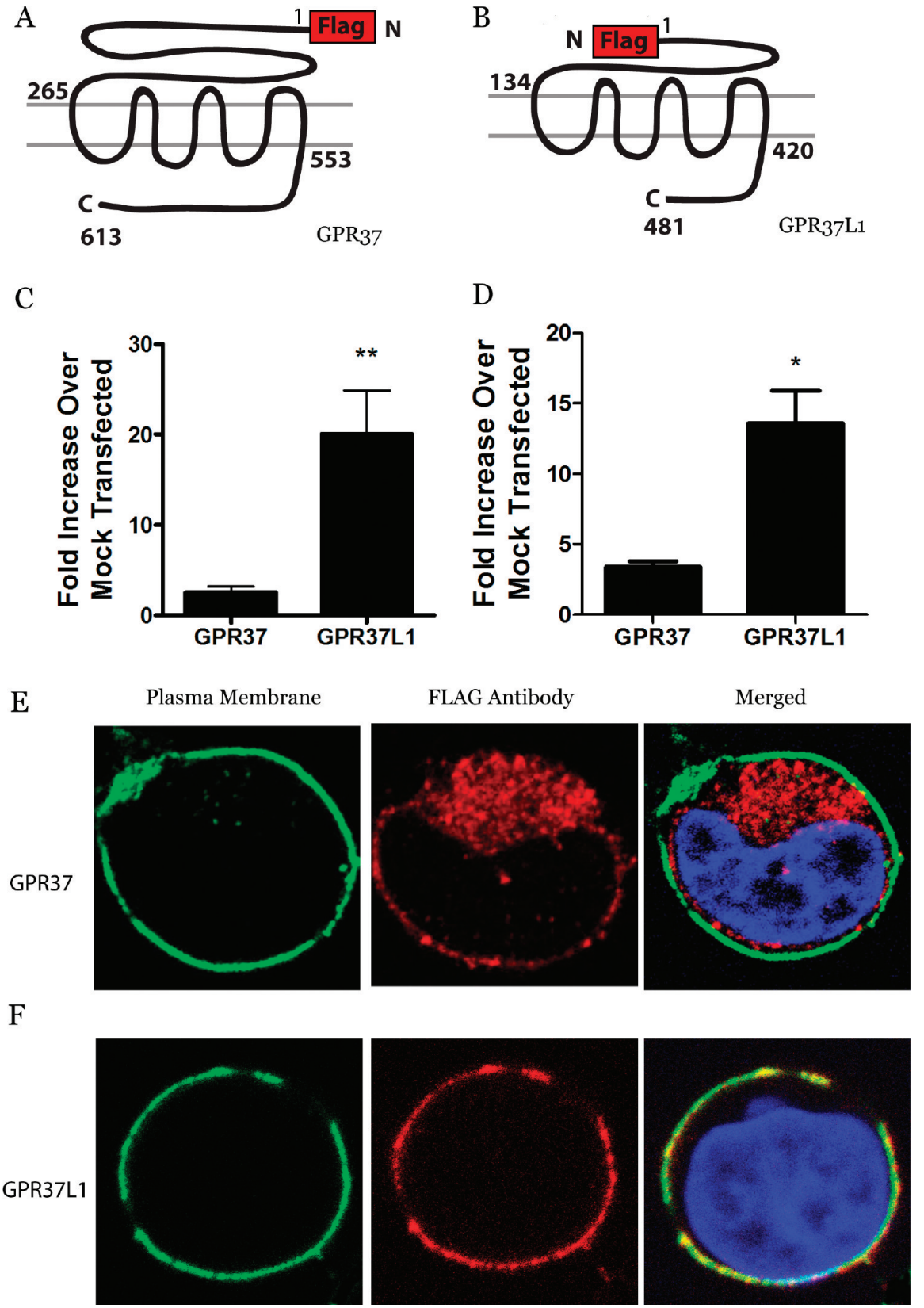

FIGURE 1: GPR37L1 exhibits robust plasma membrane expression, but GPR37 does not. GPR37 (A) and GPR37L1 (B) were transiently transfected into HEK-293 cells. Cell surface expression was assessed using a luminometer-based assay (C) and via flow cytometry (D). Values are expressed as means ± SEM for fold surface expression over mock transfected cells. Unpaired *t* tests were used to determine statistical significance ($n = 27$ and 3, respectively; $^{*}p < 0.05$, and $^{**}p < 0.005$). Confocal imaging of representative cells transfected with wt GPR37 (E) or GPR37L1 (F) was done using mouse anti-Na^{+}/K^{+} ATPase, followed by Alexa Fluor 488, to mark the cell surface (green, left panels), rabbit anti-FLAG, followed by Alexa Fluor 546, to detect the receptors (red, center panels), and DAPI to stain the nucleus (blue, right panels). Yellow indicates colocalization of the receptor with the plasma membrane (C and D, right panels).

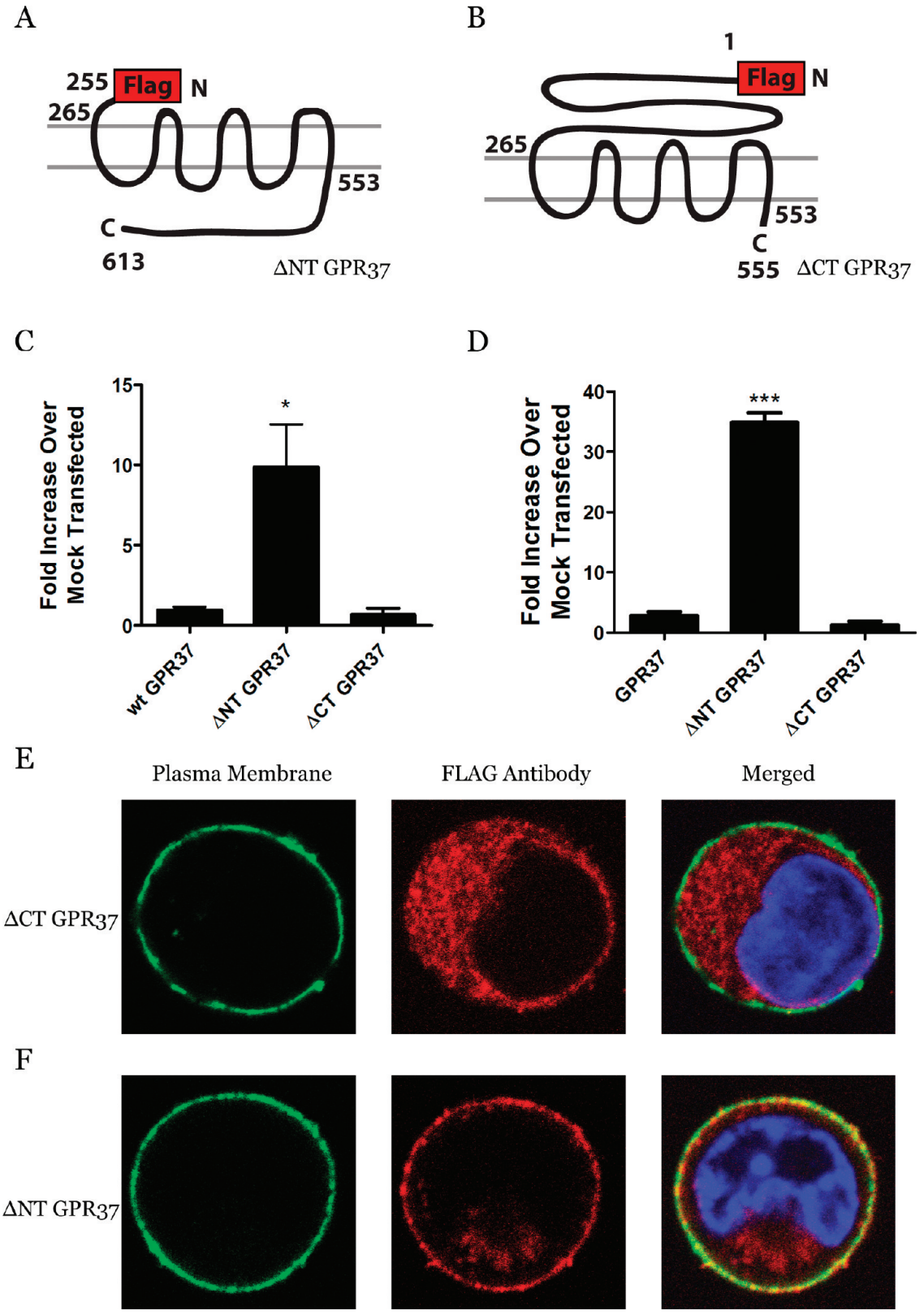

FIGURE 2: N-Terminal truncation of GPR37 enhances plasma membrane expression. Constructs corresponding to N-terminal truncation (A) and C-terminal truncation (B) of GPR37 were prepared with N-terminal FLAG tags. HEK-293 cells were transiently transfected with wt GPR37, ΔNT-GPR37, and ΔCT-GPR37. Surface expression was detected using a luminometer-based assay (C) and via flow cytometry (D). Values are expressed as means ± SEM for fold increase over wt GPR37. One-way ANOVA followed by Tukey's post hoc test was used to determine statistical significance ($n = 3-6$; *$p < 0.05$, and ***$p < 0.0001$). Confocal imaging of cells transfected with ΔCT-GPR37 (E) or ΔNT-GPR37 (F) was conducted using mouse anti-Na^+/K^+ ATPase, followed by Alexa Fluor 488, to mark the cell surface (green, left panels), rabbit anti-FLAG, followed by Alexa Fluor 546, to detect the receptors (red, center panels), and DAPI to stain the nucleus (blue, right panels). Yellow indicates colocalization of the receptor with the plasma membrane (E and F, right panels).

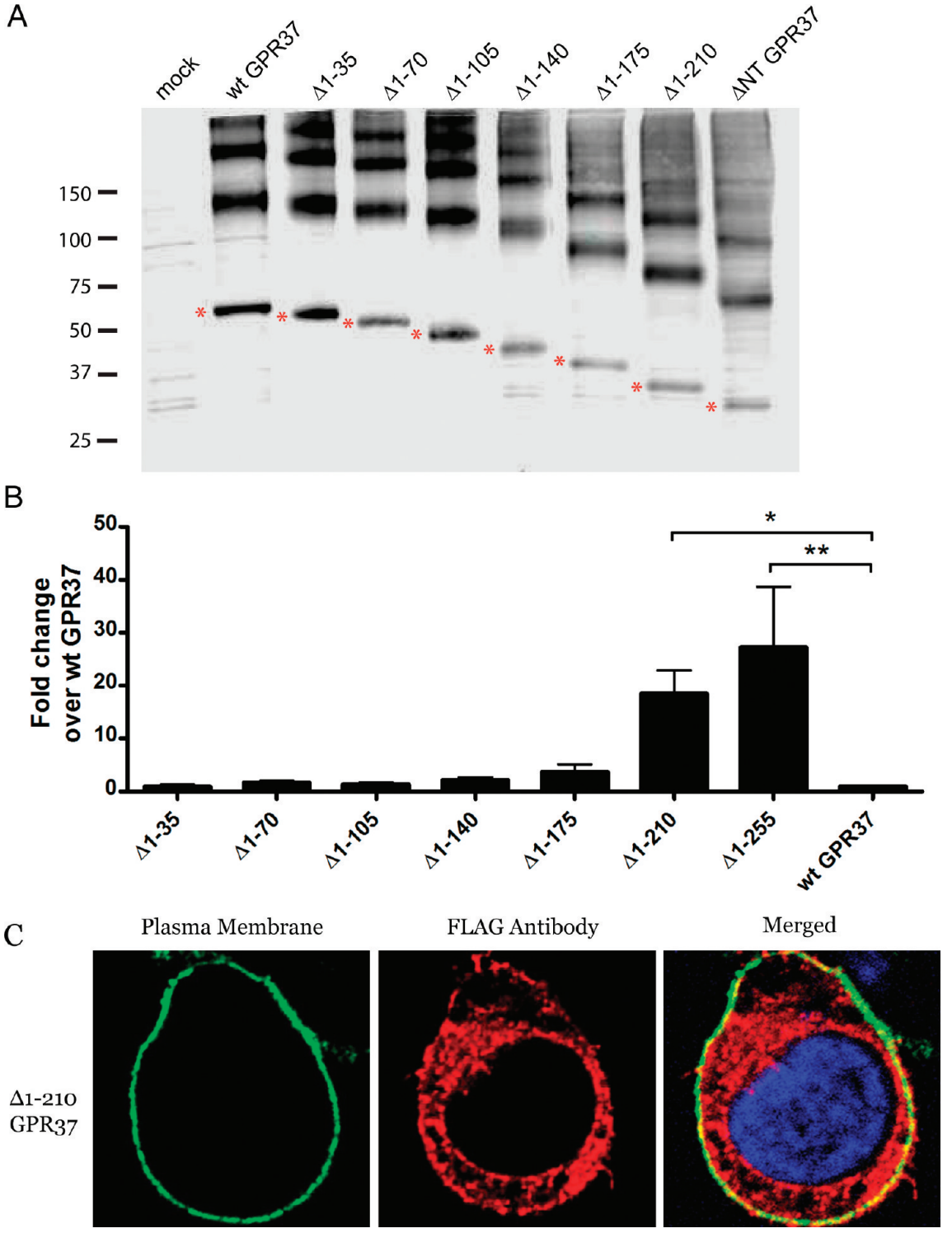

FIGURE 3: Regions on the GPR37 N-terminus influencing receptor surface expression. (A) Representative Western blot of N-terminally truncated constructs. HEK-293 cells expressing empty pCMV2b vector, wt GPR37, Δ^{1-35}, Δ^{1-70}, Δ^{1-105}, Δ^{1-140}, Δ^{1-175}, Δ^{1-210}, and ΔNT were harvested, run on SDS−PAGE gels, transferred, and blotted with anti-FLAG antibody. The monomeric species of interest is indicated with a red asterisk to the left of each band. High-molecular weight species represent aggregated receptor, as is often seen for GPR37. (B) Surface expression of these receptors was assessed using a luminometer-based assay. Values are expressed as means ± SEM for fold increase over wt GPR37. One-way ANOVA followed by Dunnett's post hoc test was used to determine statistical significance. ($n = 5$; $^*p < 0.05$, and $^{**}p < 0.01$). Confocal imaging of HEK-293 cells expressing Δ^{1-210} GPR37 (C) was done using mouse anti-Na^+/K^+ ATPase, followed by Alexa Fluor 488, to mark the cell surface (green, left panel), rabbit anti-FLAG, followed by Alexa Fluor 546, to detect the receptors (red, center panel), and DAPI to stain the nucleus (blue, right panel). Yellow indicates colocalization of the receptor with the plasma membrane (C, right panel).

diverging NT and CT sequences, we created two N-terminally FLAG-tagged truncated mutants of GPR37, one in which 255 N-terminal amino acids were deleted [ΔNT-GPR37 (Figure 2A)] and a second in which 58 C-terminal amino acids were deleted [ΔCT-GPR37 (Figure 2B)]. In the luminometer-based assay, the surface expression of ΔCT-GPR37 was observed to be equivalent to that of full-length GPR37, hereafter identified as wild-type GPR37 (wt GPR37). However, the ΔNT-GPR37 mutant ex-

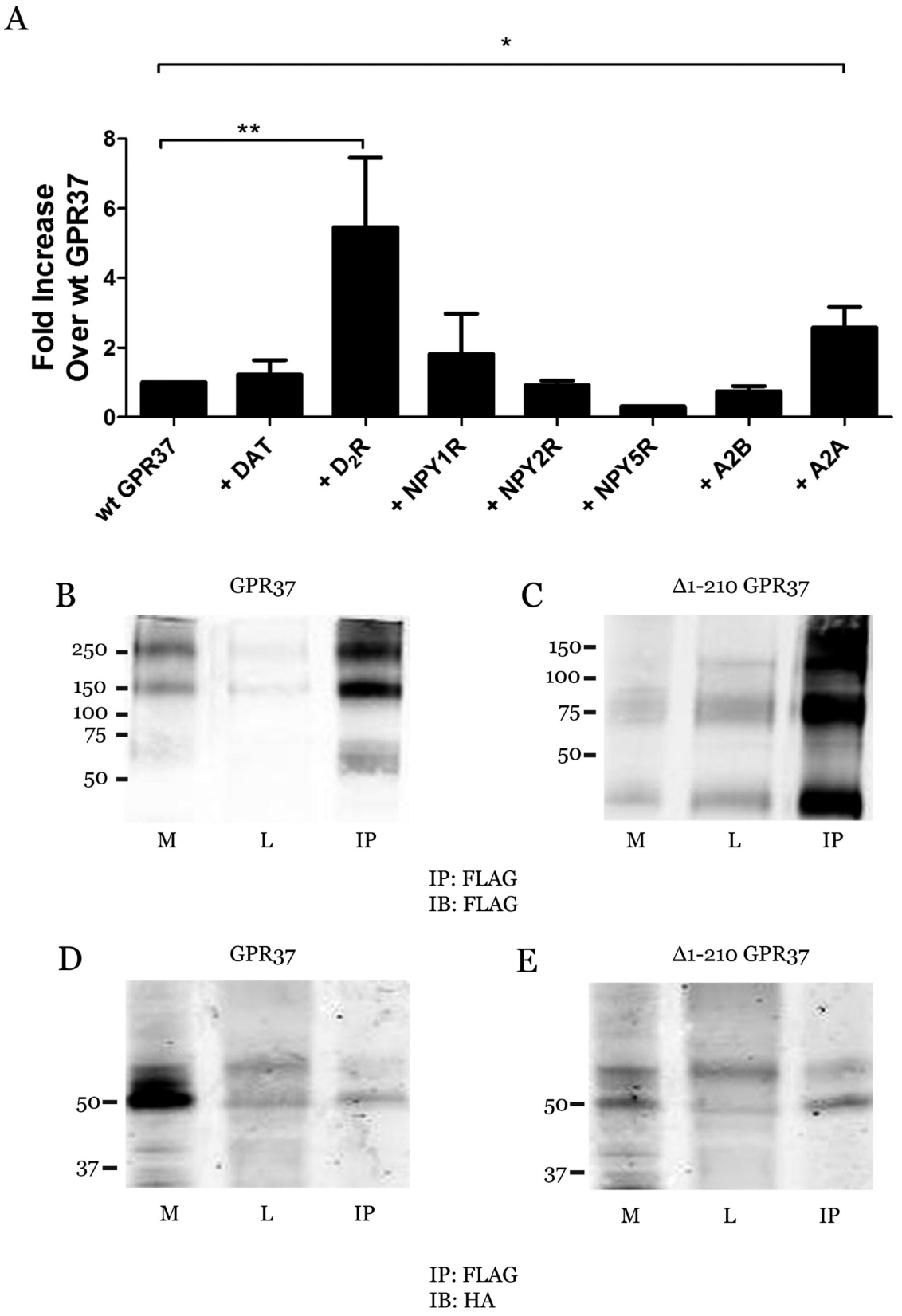

FIGURE 4: Physical association between D_2R and GPR37. HEK-293 cells were transiently transfected with FLAG-tagged GPR37 with or without DAT, HA-D_2R, HA-NPY_1, HA-NPY_2, HA-$A_{2B}R$, or HA-$A_{2A}R$. (A) Surface expression of GPR37 was assessed using a luminometer-based assay. Values are expressed as means ± the standard error of the mean for fold increase over wt GPR37. A Student's *t* test was used to determine statistical significance ($n = 3-8$; $*p < 0.05$, and $**p < 0.005$). (B–E) Cells were harvested, lysed, and immunoprecipitated (IP) with an anti-FLAG antibody. Western blot detection of membrane (M), soluble lysate (L), and IP fractions with anti-FLAG (B and C) or anti-HA antibody (D and E) revealed robust co-immunoprecipitation of D_2R with both GPR37 (B and D) and mutant Δ^{1-210} GPR37 (C and E). The D_2R was observed at its expected molecular mass of 48–52 kDa, with the different bands most likely corresponding to differentially glycosylated forms of the receptor.

Table 1: Coexpression with $\Delta^{1\text{-}210}$ GPR37 Modulates D_2R Ligand Binding Affinity[a]

	dopamine		quinpirole	
	D_2R	$D_2R-GPR37$	D_2R	$D_2R-GPR37$
$K_i \pm$ SEM (nM)	97 ± 27	41 ± 10	82 ± 38	36 ± 9

	haloperidol		spiperone		YM-09151	
	D_2R	$D_2R-GPR37$	D_2R	$D_2R-GPR37$	D_2R	$D_2R-GPR37$
$K_D/K_i \pm$ SEM (pM)	1114 ± 86	480 ± 76	72 ± 20	43 ± 10	1228 ± 567	621 ± 193

[a]Ligand binding studies were performed, as described in Materials and Methods, on membranes derived from HEK-293 cells that had been transfected to transiently express HA-D_2R in the absence and presence of FLAG-tagged Δ^{1-210} GPR37, due to the better expression of the truncated mutant of GPR37 and its robust association with D_2R. Estimates of K_i or K_D (±SEM) for each ligand are provided. For the curves of dopamine and quinpirole displacement of [^{3}H]spiperone binding, two-site fits were not significantly better than one-site fits; therefore, one-site fit values are shown.

hibited a striking increase in surface expression relative to either of the other constructs (Figure 2C). These findings were confirmed in flow cytometry experiments (Figure 2D), as well as with confocal microscopy, in which ΔCT-GPR37 exhibited the same intracellular distribution as wt GPR37 (Figure 2E), while ΔNT-GPR37 was predominantly associated with the plasma membrane (Figure 2F). Again, MATLAB analysis confirmed the qualitative observations, with ~38% of transfected ΔNT-GPR37 being expressed at the cell surface.

Regions of the GPR37 N-Terminus Control Receptor Surface Expression. The results with the ΔNT-GPR37 mutant suggested that a motif on the GPR37 NT is a critical determinant of the plasma membrane localization of GPR37. To determine the location and sequence of this potential motif, we generated six sequentially truncated constructs of GPR37 (Δ^{1-35}, Δ^{1-70}, Δ^{1-105}, Δ^{1-140}, Δ^{1-175}, and Δ^{1-210} GPR37) by removing 35 additional amino acids from the NT in each additional construct (Figure 3A). Evaluation of the cell surface expression of these constructs was performed using the luminometer-based assay. As shown in Figure 3B, very little surface expression was observed in the first four mutants, and the Δ^{1-175} mutant exhibited only a slight increase over wt GPR37. However, the Δ^{1-210} mutant exhibited a robust enhancement of cell surface expression, similar to that of ΔNT-GPR37. Confocal images revealing colocalization between Δ^{1-210} GPR37 and the Na^+/K^+ ATPase, a plasma membrane marker, confirmed the findings from the luminometer experiments (Figure 3C); analysis of the images using MATLAB revealed that approximately 25% of the overall transfected Δ^{1-210} GPR37 exhibited cell surface expression.

The *Hydra* peptide head activator (HA) has been reported to be a ligand that activates and induces internalization of GPR37 in a pertussis toxin sensitive manner, indicating that HA might promote coupling of GPR37 to $G\alpha_i$ or $G\alpha_o$ (*6*). To test if the GPR37 mutants that exhibited enhanced trafficking, ΔNT-GPR37 and Δ^{1-210} GPR37, also exhibited functional activity in response to the HA peptide, HEK-293 cells were transfected with either ΔNT, Δ^{1-210}, or wt GPR37 and then stimulated with HA. Luminometer-based surface expression assays were performed to measure HA-induced receptor internalization; phospho-ERK assays were performed to assess HA-stimulated ERK1/2 phosphorylation, and cyclic AMP assays were conducted to test for HA-induced inhibition of adenylyl cyclase activity. However, despite repeated studies with the HA peptide from different sources over a range of concentrations, we were unable to find evidence of HA-induced activation of ΔNT, Δ^{1-210}, or wt GPR37 in these studies (data not shown).

Dopamine Receptor D_2R Interacts with GPR37. Studies of other poorly transported GPCRs, such as the aforementioned $GABA_BR1$ and α_{1D}-AR, have revealed that receptor surface expression can sometimes be greatly enhanced upon coexpression with interacting GPCRs (*21*−*25*). GPR37 has been reported to associate with the dopamine transporter (DAT) (*28*), but there have not yet been any studies of possible interactions of GPR37 with other GPCRs. Thus, we coexpressed GPR37 in HEK-293 cells with DAT, as well as a handful of GPCRs that possess similar regional expression patterns in the brain, and quantified GPR37 surface expression. In comparison with GPR37 expressed alone, the luminometer-based cell surface assay revealed an increase in the level of GPR37 surface expression when coexpressed with the adenosine A_{2A} receptor, as well as a much larger increase when coexpressed with dopamine D_2R (Figure 4A). Neither DAT nor any of the other receptors ($A_{2B}R$ and neuropeptide receptors NPY_1 and NPY_2) had any effect on the surface expression of GPR37. To examine whether D_2R might form complexes with GPR37 in cells, we performed co-immunoprecipitation studies, which revealed a robust interaction between GPR37 and D_2R (Figure 4B−E). Both wt GPR37 (Figure 4D) and the Δ^{1-210} mutant (Figure 4E) co-immunoprecipitated with both the immature (unprocessed) and mature (glycosylated) forms of D_2R (bottom and top bands, respectively), indicating the interaction between these two receptors likely occurs in the ER and is maintained after glycosylation. The Δ^{1-210} mutant exhibited a consistently stronger interaction with D_2R than did wt GPR37, probably due to the enhanced plasma membrane expression of the mutant receptor. Therefore, we used the Δ^{1-210} mutant for further studies on the effects of GPR37 on D_2R properties.

Receptor−receptor interactions often modulate the endocytic trafficking of GPCRs (*22*−*25*). In some cases, interaction with a partner receptor can inhibit normal agonist-induced internalization of a given GPCR, whereas in other cases, stimulation by the ligand of one receptor can induce an interacting receptor to be co-internalized (*29*−*31*). To observe the effects of Δ^{1-210} GPR37 coexpression on the agonist-induced internalization rate of D_2R, and also to assess the possibility of Δ^{1-210} GPR37 co-internalization upon D_2R agonist stimulation, luminometer-based surface expression assays were conducted. Upon treatment with the D_2R agonist quinpirole for 30 min, the individually expressed D_2R was internalized by 32 ± 9%. Similarly, when coexpressed with Δ^{1-210} GPR37, quinpirole-stimulated D_2R was internalized by 33 ± 2%. Co-internalization of Δ^{1-210} GPR37 was not observed upon coexpression with D_2R and quinpirole stimulation, and

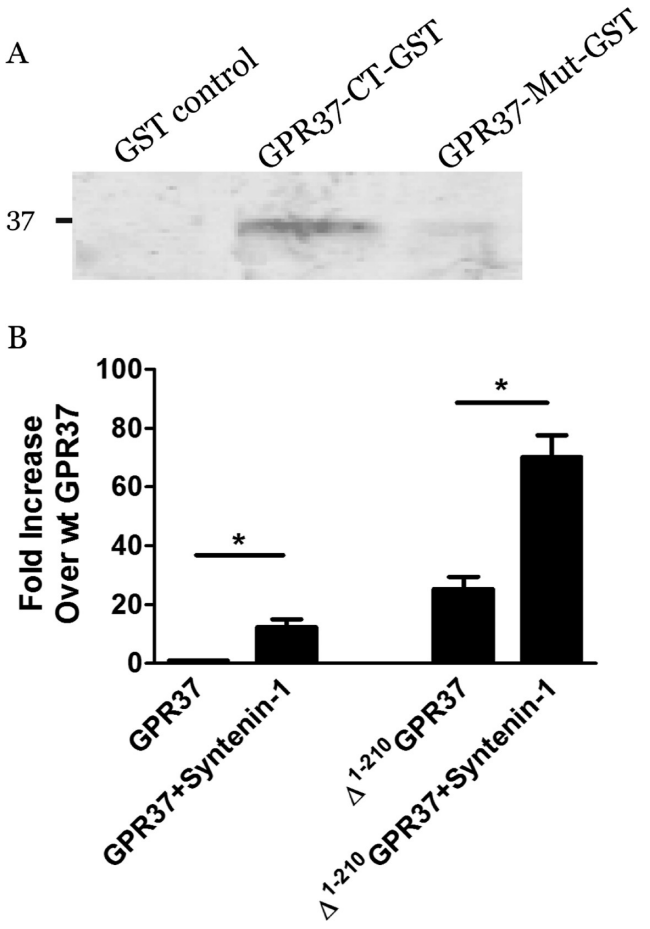

FIGURE 5: Physical association between GPR37 and syntenin-1. (A) Pull-down studies were performed via examination of interactions of syntenin-1 with control GST, the GPR37-CT−GST fusion protein, and a mutant version of the GPR37-CT−GST fusion protein (GPR37-Mut−GST) with the PDZ-binding motif removed. Robust binding of syntenin-1 was observed only with wild-type GPR37-CT−GST fusion protein. (B) HEK-293 cells were transiently transfected with wt GPR37 or Δ^{1-210} GPR37 in the absence and presence of coexpressed HA-syntenin-1. Surface expression of the receptors was assessed using a luminometer-based assay. Values are expressed as means ± SEM and as the fold increase over wt GPR37 alone ($n = 3-4$; $^*p < 0.05$).

co-immunoprecipitation experiments performed in the absence and presence of quinpirole treatment revealed that the interaction between D_2R and GPR37 was unchanged upon agonist stimulation (data not shown). Thus, we found no evidence of agonist regulation of the interaction, and also no evidence that the interaction altered agonist-promoted internalization of D_2R.

Coexpression with Δ^{1-210} GPR37 Alters D_2R Ligand Binding Properties. To determine if the physical interaction between GPR37 and D_2R might have effects on D_2R functionality, ligand binding studies were performed using radiolabeled versions of the D_2R antagonists spiperone and YM-09151. Both ligands exhibited modest but significant increases in affinity for D_2R when D_2R was coexpressed with Δ^{1-210} GPR37 (Table 1). Competition curves were also determined for displacement of [^{3}H]spiperone binding by unlabeled versions of the D_2R agonists dopamine and quinpirole and the D_2R antagonist haloperidol. The affinities of these ligands for D_2R were also somewhat altered when D_2R was coexpressed with Δ^{1-210} GPR37, with the magnitude of the change being ligand-specific (Table 1). To investigate whether these differences in ligand binding might correspond to changes in functional activity, [^{35}S]GTPγS binding studies were performed on membranes derived from cells overexpressing $G\alpha_o$ protein and D_2R in the absence and presence of Δ^{1-210} GPR37. However, no significant shift in EC_{50} was observed when Δ^{1-210} GPR37 was coexpressed with D_2R, compared to D_2R alone (data not shown).

Coexpression of GPR37 with Syntenin-1 Enhances GPR37 Surface Expression. The GPR37 CT possesses a consensus class 1 PDZ domain-binding motif (G-T-H-C). To examine whether GPR37 might interact via this motif with PDZ domain-containing scaffold proteins, we prepared the GPR37 CT as a GST fusion protein and screened it against a proteomic array of 96 purified PDZ domains (*32*, *33*). However, the GPR37-CT−GST fusion protein did not exhibit detectable binding to any of the PDZ domains on the array (data not shown). In addition to this proteomic approach toward searching for GPR37-interacting partners, we also took a bioinformatics approach and noted that GPR37 terminates in precisely the same C-terminal motif as the glycine transporter GlyT2 (G-T-x-C). Since GlyT2 has been shown to interact via this motif with the atypical PDZ scaffold syntenin-1 (*34*, *35*), which is not included in our array, we specifically examined whether GPR37 and syntenin-1 might interact. As shown in Figure 5A, pull-down analyses revealed a robust interaction between the GPR37-CT−GST fusion protein and syntenin-1. This interaction was not seen using a mutated version of the GPR37-CT−GST fusion protein (GPR37-Mut−GST), in which the final cysteine residue had been removed to disrupt the PDZ-binding motif. Moreover, when syntenin-1 was coexpressed with full-length GPR37 in HEK-293 cells, the result was a striking 10-fold increase in the amount of GPR37 that could be detected in the plasma membrane (Figure 5B). Interestingly, coexpression of syntenin-1 with Δ^{1-210} GPR37 still resulted in a 3-fold increase in the level of surface expression of the truncated mutant receptor, revealing that a combination of approaches (truncation of the receptor's NT and coexpression of the receptor with a CT-binding partner) can work synergistically to maximize trafficking of GPR37 to the plasma membrane in heterologous cells (Figure 5B).

DISCUSSION

Most GPCRs must reach the plasma membrane to achieve proper functional activity. Thus, the identification of ligands for orphan GPCRs can be greatly impeded if the receptors exhibit trafficking defects when expressed in heterologous cells. For this reason, we sought to find ways to enhance the surface trafficking of GPR37, an orphan receptor that is well-known to suffer from trafficking defects upon heterologous expression (*1*, *6*, *8*, *27*). We have identified three distinct approaches by which trafficking of GPR37 to the plasma membrane can be enhanced: truncation of the receptor's N-terminus, coexpression with certain GPCRs, and coexpression with the PDZ scaffold syntenin-1.

The effects of truncating the N-terminus of GPR37 are similar to the effects of N-terminal truncations on the surface trafficking of the CB1 cannabinoid receptor (*16*, *36*) and the α_{1D}-adrenergic receptor (*17*−*20*). For both of these receptors, N-terminal truncations greatly improve receptor surface expression, although it is not certain if the receptors' N-termini possess specific ER retention motifs that are removed by the truncations or if instead there are global difficulties in folding that are

resolved through the removal of hard-to-fold regions. It is unlikely that removal of glycosylation sites could account for the observed effects of N-terminal truncation in our studies, since removal of glycosylation sites almost invariably causes impairment in the surface expression of GPCRs rather than enhancement (*37*−*40*). Indeed, there are three putative sites of N-linked glycosylation sites on the NT of GPR37, but none of these sites is found between amino acids 175 and 210, which we determined to be the critical region for determining the receptor's surface expression.

After observing that N-terminal truncations could greatly enhance GPR37 surface trafficking in heterologous cells, we sought to determine if the surface-expressed truncated mutant versions of GPR37 were functionally active. Since the *Hydra* peptide head activator (HA) has been reported to be an agonist for GPR37, we explored potential HA-mediated stimulation of wt GPR37 and the truncated versions of GPR37. However, in a variety of assays under a variety of different conditions, we were unable to detect any evidence of HA-induced activation of GPR37, GPR37L1, or any of the mutant versions of GPR37 that we had created. It is possible, of course, that truncations of the GPR37 N-terminus might destroy the binding site for HA, but comparable N-terminal truncations to the endothelin B receptor, the receptor most closely related to GPR37 and GPR37L1, do not disrupt ligand binding (*41*, *42*). Thus, there is reason to believe that the truncated GPR37 mutants still may be functionally active. As for our studies on full-length GPR37, the discrepancy between the positive findings of Rezgaoui et al. (*6*) and our negative findings for HA stimulation of wild-type GPR37 might be explained by differences in the cell lines used or other technical factors. Regardless of the explanation, it seems that GPR37 and GPR37L1 should still be considered as orphan receptors at present, especially since it is not clear that a peptide similar to HA exists in vertebrates. Though there were a handful of papers several decades ago reporting HA-like immunoreactivity in sections of mammalian brains (*43*−*45*), there have not been any positive follow-up studies in the past 20 years to confirm these early observations.

In addition to truncations to the GPR37 N-terminus, we found a second approach that resulted in enhanced GPR37 surface expression in heterologous cells, coexpression with certain other GPCRs, notably the dopamine D_2 receptor and adenosine A_{2A} receptor. Interestingly, D_2R and $A_{2A}R$ are known to be capable of functional interactions with each other and are also known to be found abundantly in the striatum (*46*), a brain region where GPR37 is strongly expressed (*2*, *47*). Many studies on cross-talk between D_2R and $A_{2A}R$ have focused on how stimulation of one of the receptors can directly influence the properties of the other partner (*46*). However, in the absence of a functional ligand for GPR37, such cross-talk studies on the putative heterodimers (GPR37−D_2R and GPR37−$A_{2A}R$) are not possible at present. Thus, we focused on determining whether coexpression with GPR37 might alter the properties of D_2R.

In ligand binding studies, we found that coexpression with GPR37 induced modest shifts in the affinity of D_2R for various ligands. Although these shifts were only in the range of 1.5−2.5-fold, the true magnitude of the changes may be underestimated in our studies, since our transfection efficiency was not 100%. Moreover, it is unlikely that there would be 100% efficient coassembly of the receptors even in cells that were doubly transfected with D_2R and GPR37. Thus, any observed changes in the properties of the D_2R−GPR37 heterodimer relative to D_2R alone would likely be underestimated in coexpression studies of this type. As for the potential in vivo relevance of the effects of GPR37 on D_2R properties, it is interesting to note that the affinity of D_2R for [^{3}H]YM-09151-2 in GPR37 knockout mice is decreased by approximately 2-fold (*28*), which is strikingly consistent with the approximately 2-fold increase in the affinity of D_2R for [^{3}H]YM-09151-2 that we observed upon cotransfection of D_2R with GPR37. If it is true that associations between GPR37 and D_2R can subtly influence D_2R antagonist binding properties in vivo, this is a point of significant clinical interest given the widespread use of D_2R antagonists in treating schizophrenia (*48*). Since GPR37 is coexpressed in vivo with D_2R in some neuronal populations but not others (*47*), it may be possible to develop D_2R antagonists with enhanced regional selectivity by developing compounds that preferentially target the D_2R−GPR37 complex relative to D_2R alone (or vice versa).

The third and final approach that we found to result in enhanced surface expression of GPR37 was coexpression with the PDZ scaffold syntenin-1. These findings are similar to previous observations that surface trafficking of the α_{1D}-adrenergic receptor can be strongly promoted by interactions of the receptor with a distinct class of PDZ scaffolds, the syntrophins (*49*, *50*). The interaction of GPR37 with syntenin-1 was quite specific, as screens of a proteomic array consisting of 96 other PDZ domains with the CT of GPR37 did not reveal detectable interactions with any other PDZ domains. GPR37 terminates in a motif, G-T-x-C, that is identical to the motif found at the C-terminus of the syntenin-1 binding partner GlyT2 (*34*, *35*). For GlyT2, the primary functional consequence of interaction with syntenin-1 is enhanced trafficking to synapses (*35*). For several other syntenin-1-interacting proteins, including pro-transforming growth factor α (*51*), CD63 (*52*), and the Notch ligand Delta1 (*53*), coexpression with syntenin-1 has been shown to markedly enhance trafficking to the plasma membrane, similar to the effects on GPR37 that we observed in our studies. Interestingly, syntenin-1 is known to be strongly expressed in oligodendrocytes (*54*), the cell type in which GPR37 is most abundantly expressed (*1*). Since GPR37 is an orphan receptor, it is not possible at present to test whether the GPR37−syntenin-1 association has effects on the receptor's functional properties, but the dramatic effects of syntenin-1 on GPR37 surface expression may prove to be useful in screens for potential GPR37 ligands that would allow for deorphanization of the receptor.

In summary, we have elucidated three distinct approaches by which the trafficking of GPR37 to the plasma membrane can be enhanced. Moreover, we have shown that GPR37L1, a close relative of GPR37, exhibits robust surface expression in heterologous cells. Thus, if it is assumed that GPR37 and GPR37L1 are activated by the same ligand, or at least related ligands, it seems that GPR37L1 might prove to be the superior choice for screens attempting to identify the ligand(s) for this orphan receptor pair. However, screens focused solely on GPR37 may benefit from application of one or several of the approaches described here, including N-terminal truncation, coexpression with partner receptors, and/or coexpression with syntenin-1, to achieve improved surface trafficking and enhanced functionality of GPR37. Furthermore, when more is known about the ligand binding and signaling capabilities of GPR37, the interactions described here between GPR37 and other receptors and the GPR37−syntenin-1 complex may eventually help to shed light on the regulation of GPR37 functional activity in vivo.

ACKNOWLEDGMENT

We thank Heide Oller for her help in the construction of several constructs used in these studies. We also thank Howard Rees for his guidance with the confocal microscope, Richard Dunham for his help with flow cytometry, and Cristina Bush for her assistance with the luminometer-based surface assays. In addition, we thank Paul Coffer for providing the HA-syntenin-1 construct, Gary Miller for the DAT construct, and Daniela Marazziti for her suggestions, guidance, and discussion.

REFERENCES

1. Imai, Y., Soda, M., Inoue, H., Hattori, N., Mizuno, Y., and Takahashi, R. (2001) An unfolded putative transmembrane polypeptide, which can lead to endoplasmic reticulum stress, is a substrate of Parkin. *Cell 105*, 891–902.
2. Zeng, Z., Su, K., Kyaw, H., and Li, Y. (1997) A novel endothelin receptor type-B-like gene enriched in the brain. *Biochem. Biophys. Res. Commun. 233*, 559–567.
3. Leng, N., Gu, G., Simerly, R. B., and Spindel, E. R. (1999) Molecular cloning and characterization of two putative G protein-coupled receptors which are highly expressed in the central nervous system. *Brain Res. Mol. Brain Res. 69*, 73–83.
4. Marazziti, D., Golini, E., Gallo, A., Lombardi, M. S., Matteoni, R., and Tocchini-Valentini, G. P. (1997) Cloning of GPR37, a gene located on chromosome 7 encoding a putative G-protein-coupled peptide receptor, from a human frontal brain EST library. *Genomics 45*, 68–77.
5. Valdenaire, O., Giller, T., Breu, V., Ardati, A., Schweizer, A., and Richards, J. G. (1998) A new family of orphan G protein-coupled receptors predominantly expressed in the brain. *FEBS Lett. 424*, 193–196.
6. Rezgaoui, M., Susens, U., Ignatov, A., Gelderblom, M., Glassmeier, G., Franke, I., Urny, J., Imai, Y., Takahashi, R., and Schaller, H. C. (2006) The neuropeptide head activator is a high-affinity ligand for the orphan G-protein-coupled receptor GPR37. *J. Cell Sci. 119*, 542–549.
7. Imai, Y., Soda, M., Hatakeyama, S., Akagi, T., Hashikawa, T., Nakayama, K. I., and Takahashi, R. (2002) CHIP is associated with Parkin, a gene responsible for familial Parkinson's disease, and enhances its ubiquitin ligase activity. *Mol. Cell 10*, 55–67.
8. Kubota, K., Niinuma, Y., Kaneko, M., Okuma, Y., Sugai, M., Omura, T., Uesugi, M., Uehara, T., Hosoi, T., and Nomura, Y. (2006) Suppressive effects of 4-phenylbutyrate on the aggregation of Pael receptors and endoplasmic reticulum stress. *J. Neurochem. 97*, 1259–1268.
9. Marazziti, D., Di Pietro, C., Golini, E., Mandillo, S., Matteoni, R., and Tocchini-Valentini, G. P. (2009) Induction of macroautophagy by overexpression of the Parkinson's disease-associated GPR37 receptor. *FASEB J. 23*, 1–10.
10. Marazziti, D., Golini, E., Mandillo, S., Magrelli, A., Witke, W., Matteoni, R., and Tocchini-Valentini, G. P. (2004) Altered dopamine signaling and MPTP resistance in mice lacking the Parkinson's disease-associated GPR37/parkin-associated endothelin-like receptor. *Proc. Natl. Acad. Sci. U.S.A. 101*, 10189–10194.
11. Couve, A., Filippov, A. K., Connolly, C. N., Bettler, B., Brown, D. A., and Moss, S. J. (1998) Intracellular retention of recombinant GABAB receptors. *J. Biol. Chem. 273*, 26361–26367.
12. Calver, A. R., Robbins, M. J., Cosio, C., Rice, S. Q., Babbs, A. J., Hirst, W. D., Boyfield, I., Wood, M. D., Russell, R. B., Price, G. W., Couve, A., Moss, S. J., and Pangalos, M. N. (2001) The C-terminal domains of the GABA(b) receptor subunits mediate intracellular trafficking but are not required for receptor signaling. *J. Neurosci. 21*, 1203–1210.
13. Margeta-Mitrovic, M., Jan, Y. N., and Jan, L. Y. (2000) A trafficking checkpoint controls GABA(B) receptor heterodimerization. *Neuron 27*, 97–106.
14. Margeta-Mitrovic, M., Mitrovic, I., Riley, R. C., Jan, L. Y., and Basbaum, A. I. (1999) Immunohistochemical localization of GABA-(B) receptors in the rat central nervous system. *J. Comp. Neurol. 405*, 299–321.
15. Pagano, A., Rovelli, G., Mosbacher, J., Lohmann, T., Duthey, B., Stauffer, D., Ristig, D., Schuler, V., Meigel, I., Lampert, C., Stein, T., Prezeau, L., Blahos, J., Pin, J., Froestl, W., Kuhn, R., Heid, J., Kaupmann, K., and Bettler, B. (2001) C-Terminal interaction is essential for surface trafficking but not for heteromeric assembly of GABA(b) receptors. *J. Neurosci. 21*, 1189–1202.
16. Andersson, H., D'Antona, A. M., Kendall, D. A., Von Heijne, G., and Chin, C. N. (2003) Membrane assembly of the cannabinoid receptor 1: Impact of a long N-terminal tail. *Mol. Pharmacol. 64*, 570–577.
17. Hague, C., Chen, Z., Pupo, A. S., Schulte, N. A., Toews, M. L., and Minneman, K. P. (2004) The N terminus of the human α1D-adrenergic receptor prevents cell surface expression. *J. Pharmacol. Exp. Ther. 309*, 388–397.
18. Hague, C., Uberti, M. A., Chen, Z., Hall, R. A., and Minneman, K. P. (2004) Cell surface expression of α1D-adrenergic receptors is controlled by heterodimerization with α1B-adrenergic receptors. *J. Biol. Chem. 279*, 15541–15549.
19. Pupo, A. S., Uberti, M. A., and Minneman, K. P. (2003) N-Terminal truncation of human α1D-adrenoceptors increases expression of binding sites but not protein. *Eur. J. Pharmacol. 462*, 1–8.
20. Uberti, M. A., Hall, R. A., and Minneman, K. P. (2003) Subtype-specific dimerization of α1-adrenoceptors: Effects on receptor expression and pharmacological properties. *Mol. Pharmacol. 64*, 1379–1390.
21. Dunham, J. H., and Hall, R. A. (2009) Enhancement of the surface expression of G protein-coupled receptors. *Trends Biotechnol. 27*, 541–545.
22. Prinster, S. C., Hague, C., and Hall, R. A. (2005) Heterodimerization of g protein-coupled receptors: Specificity and functional significance. *Pharmacol. Rev. 57*, 289–298.
23. Bulenger, S., Marullo, S., Chen, Z., and Bouvier, M. (2005) Emerging role of homo- and heterodimerization in G-protein-coupled receptor biosynthesis and maturation. *Trends Pharmacol. Sci. 26*, 131–137.
24. Ferre, S., Quiroz, C., Woods, A. S., Cunha, R., Popoli, P., Ciruela, F., Lluis, C., Franco, R., Azdad, K., and Schiffmann, S. N. (2008) An update on adenosine A2A-dopamine D2 receptor interactions: Implications for the function of G protein-coupled receptors. *Curr. Pharm. Des. 14*, 1468–1474.
25. Milligan, G. (2009) G protein-coupled receptor hetero-dimerization: Contribution to pharmacology and function. *Br. J. Pharmacol. 158*, 5–14.
26. Weinman, E. J., Hall, R. A., Friedman, P. A., Liu-Chen, L. Y., and Shenolikar, S. (2006) The association of NHERF adaptor proteins with G protein-coupled receptors and receptor tyrosine kinases. *Annu. Rev. Physiol. 68*, 491–505.
27. Yang, Y., Nishimura, I., Imai, Y., Takahashi, R., and Lu, B. (2003) Parkin suppresses dopaminergic neuron-selective neurotoxicity induced by Pael-R in *Drosophila*. *Neuron 37*, 911–924.
28. Marazziti, D., Mandillo, S., Di Pietro, C., Golini, E., Matteoni, R., and Tocchini-Valentini, G. P. (2007) GPR37 associates with the dopamine transporter to modulate dopamine uptake and behavioral responses to dopaminergic drugs. *Proc. Natl. Acad. Sci. U.S.A. 104*, 9846–9851.
29. He, L., Fong, J., von Zastrow, M., and Whistler, J. L. (2002) Regulation of opioid receptor trafficking and morphine tolerance by receptor oligomerization. *Cell 108*, 271–282.
30. Lavoie, C., Mercier, J. F., Salahpour, A., Umapathy, D., Breit, A., Villeneuve, L. R., Zhu, W. Z., Xiao, R. P., Lakatta, E. G., Bouvier, M., and Hebert, T. E. (2002) $\beta1/\beta2$-adrenergic receptor heterodimerization regulates $\beta2$-adrenergic receptor internalization and ERK signaling efficacy. *J. Biol. Chem. 277*, 35402–35410.
31. Uberti, M. A., Hague, C., Oller, H., Minneman, K. P., and Hall, R. A. (2005) Heterodimerization with $\beta2$-adrenergic receptors promotes surface expression and functional activity of α1D-adrenergic receptors. *J. Pharmacol. Exp. Ther. 313*, 16–23.
32. Fam, S. R., Paquet, M., Castleberry, A. M., Oller, H., Lee, C. J., Traynelis, S. F., Smith, Y., Yun, C. C., and Hall, R. A. (2005) P2Y1 receptor signaling is controlled by interaction with the PDZ scaffold NHERF-2. *Proc. Natl. Acad. Sci. U.S.A. 102*, 8042–8047.
33. He, J., Bellini, M., Inuzuka, H., Xu, J., Xiong, Y., Yang, X., Castleberry, A. M., and Hall, R. A. (2006) Proteomic analysis of $\beta1$-adrenergic receptor interactions with PDZ scaffold proteins. *J. Biol. Chem. 281*, 2820–2827.
34. Ohno, K., Koroll, M., El Far, O., Scholze, P., Gomeza, J., and Betz, H. (2004) The neuronal glycine transporter 2 interacts with the PDZ domain protein syntenin-1. *Mol. Cell. Neurosci. 26*, 518–529.
35. Armsen, W., Himmel, B., Betz, H., and Eulenburg, V. (2007) The C-terminal PDZ-ligand motif of the neuronal glycine transporter GlyT2 is required for efficient synaptic localization. *Mol. Cell. Neurosci. 36*, 369–380.
36. Nordstrom, R., and Andersson, H. (2006) Amino-terminal processing of the human cannabinoid receptor 1. *J. Recept. Signal Transduction Res. 26*, 259–267.

37. He, J., Xu, J., Castleberry, A. M., Lau, A. G., and Hall, R. A. (2002) Glycosylation of β_1-adrenergic receptors regulates receptor surface expression and dimerization. *Biochem. Biophys. Res. Commun. 297*, 565–572.
38. Alken, M., Schmidt, A., Rutz, C., Furkert, J., Kleinau, G., Rosenthal, W., and Schulein, R. (2009) The sequence after the signal peptide of the G protein-coupled endothelin B receptor is required for efficient translocon gating at the endoplasmic reticulum membrane. *Mol. Pharmacol. 75*, 801–811.
39. Deslauriers, B., Ponce, C., Lombard, C., Larguier, R., Bonnafous, J. C., and Marie, J. (1999) N-Glycosylation requirements for the AT1a angiotensin II receptor delivery to the plasma membrane. *Biochem. J. 339* (Part 2), 397–405.
40. Davis, D., Liu, X., and Segaloff, D. L. (1995) Identification of the sites of N-linked glycosylation on the follicle-stimulating hormone (FSH) receptor and assessment of their role in FSH receptor function. *Mol. Endocrinol. 9*, 159–170.
41. Klammt, C., Srivastava, A., Eifler, N., Junge, F., Beyermann, M., Schwarz, D., Michel, H., Doetsch, V., and Bernhard, F. (2007) Functional analysis of cell-free-produced human endothelin B receptor reveals transmembrane segment 1 as an essential area for ET-1 binding and homodimer formation. *FEBS J. 274*, 3257–3269.
42. Doi, T., Hiroaki, Y., Arimoto, I., Fujiyoshi, Y., Okamoto, T., Satoh, M., and Furuichi, Y. (1997) Characterization of human endothelin B receptor and mutant receptors expressed in insect cells. *Eur. J. Biochem. 248*, 139–148.
43. Bodenmuller, H., and Schaller, H. C. (1981) Conserved amino acid sequence of a neuropeptide, the head activator, from coelenterates to humans. *Nature 293*, 579–580.
44. Bodenmuller, H., Schaller, H. C., and Darai, G. (1980) Human hypothalamus and intestine contain a hydra-neuropeptide. *Neurosci. Lett. 16*, 71–74.
45. Ekman, R., Salford, L., Brun, A., and Larsson, I. (1990) Hydra head activator-like immunoreactivity in human brain astrocytomas grade III-IV and the surrounding brain tissue. *Peptides 11*, 271–275.
46. Fuxe, K., Ferre, S., Genedani, S., Franco, R., and Agnati, L. F. (2007) Adenosine receptor-dopamine receptor interactions in the basal ganglia and their relevance for brain function. *Physiol. Behav. 92*, 210–217.
47. Lein, E. S., Hawrylycz, M. J., Ao, N., Ayres, M., Bensinger, A., Bernard, A., Boe, A. F., Boguski, M. S., Brockway, K. S., Byrnes, E. J., Chen, L., Chen, T. M., Chin, M. C., Chong, J., Crook, B. E., Czaplinska, A., Dang, C. N., Datta, S., Dee, N. R., Desaki, A. L., Desta, T., Diep, E., Dolbeare, T. A., Donelan, M. J., Dong, H. W., Dougherty, J. G., Duncan, B. J., Ebbert, A. J., Eichele, G., Estin, L. K., Faber, C., Facer, B. A., Fields, R., Fischer, S. R., Fliss, T. P., Frensley, C., Gates, S. N., Glattfelder, K. J., Halverson, K. R., Hart, M. R., Hohmann, J. G., Howell, M. P., Jeung, D. P., Johnson, R. A., Karr, P. T., Kawal, R., Kidney, J. M., Knapik, R. H., Kuan, C. L., Lake, J. H., Laramee, A. R., Larsen, K. D., Lau, C., Lemon, T. A., Liang, A. J., Liu, Y., Luong, L. T., Michaels, J., Morgan, J. J., Morgan, R. J., Mortrud, M. T., Mosqueda, N. F., Ng, L. L., Ng, R., Orta, G. J., Overly, C. C., Pak, T. H., Parry, S. E., Pathak, S. D., Pearson, O. C., Puchalski, R. B., Riley, Z. L., Rockett, H. R., Rowland, S. A., Royall, J. J., Ruiz, M. J., Sarno, N. R., Schaffnit, K., Shapovalova, N. V., Sivisay, T., Slaughterbeck, C. R., Smith, S. C., Smith, K. A., Smith, B. I., Sodt, A. J., Stewart, N. N., Stumpf, K. R., Sunkin, S. M., Sutram, M., Tam, A., Teemer, C. D., Thaller, C., Thompson, C. L., Varnam, L. R., Visel, A., Whitlock, R. M., Wohnoutka, P. E., Wolkey, C. K., Wong, V. Y., Wood, M., Yaylaoglu, M. B., Young, R. C., Youngstrom, B. L., Yuan, X. F., Zhang, B., Zwingman, T. A., and Jones, A. R. (2007) Genome-wide atlas of gene expression in the adult mouse brain. *Nature 445*, 168–176.
48. Strange, P. G. (2008) Antipsychotic drug action: Antagonism, inverse agonism or partial agonism. *Trends Pharmacol. Sci. 29*, 314–321.
49. Lyssand, J. S., DeFino, M. C., Tang, X. B., Hertz, A. L., Feller, D. B., Wacker, J. L., Adams, M. E., and Hague, C. (2008) Blood pressure is regulated by an α1D-adrenergic receptor/dystrophin signalosome. *J. Biol. Chem. 283*, 18792–18800.
50. Chen, Z., Hague, C., Hall, R. A., and Minneman, K. P. (2006) Syntrophins regulate α1D-adrenergic receptors through a PDZ domain-mediated interaction. *J. Biol. Chem. 281*, 12414–12420.
51. Fernandez-Larrea, J., Merlos-Suarez, A., Urena, J. M., Baselga, J., and Arribas, J. (1999) A role for a PDZ protein in the early secretory pathway for the targeting of proTGF-α to the cell surface. *Mol. Cell 3*, 423–433.
52. Latysheva, N., Muratov, G., Rajesh, S., Padgett, M., Hotchin, N. A., Overduin, M., and Berditchevski, F. (2006) Syntenin-1 is a new component of tetraspanin-enriched microdomains: Mechanisms and consequences of the interaction of syntenin-1 with CD63. *Mol. Cell. Biol. 26*, 7707–7718.
53. Estrach, S., Legg, J., and Watt, F. M. (2007) Syntenin mediates Delta1-induced cohesiveness of epidermal stem cells in culture. *J. Cell Sci. 120*, 2944–2952.
54. Chatterjee, N., Stegmuller, J., Schatzle, P., Karram, K., Koroll, M., Werner, H. B., Nave, K. A., and Trotter, J. (2008) Interaction of syntenin-1 and the NG2 proteoglycan in migratory oligodendrocyte precursor cells. *J. Biol. Chem. 283*, 8310–8317.